FINAL REPORT

Title:	"Molecular-Level Design of Heterogeneous Chiral Catalysis"
DOE Grant No.:	DE-FG02-03ER15472
Principal Investigators:	Prof. Francisco Zaera (Univ. of California, Riverside), PI Prof. Andrew Gellman (Carnegie Mellon University), Co-PI Prof. David Sholl (Carnegie Mellon University), Co-PI Prof. Wilfred T. Tysoe (Univ. of Wisconsin, Milwaukee), Co-PI
External PI:	Leonard Mueller (UC Riverside) Larry Mink (California State University, San Bernardino) Prof. Giorgio Zgrablich (Univ. of San Luis, Argentina) Prof. Dilano Saldin (Univ. of Wisconsin, Milwaukee) Prof. Carol Hirschmugl (Univ. of Wisconsin, Milwaukee)
Post-doctoral Associates:	Ilkeun Lee
Students:	Jingfeng Lai (UCR) Ryan A. Olsen (UC Riverside) (graduated) Zhen Ma (UCR) (graduated) Luke Burkholder (UWM) Lulu Tian (UWM) Jorge Boscoboinik (UWM) Yilin Wang (UWM) Jeong-Woo Han (CMU) Joanna James (CMU) Wai Yeng Cheong (CMU) Ye Huang (CMU) Sarthak Jain (CMU) Nikunj Dangaria (CMU)
Main Location:	Dept. Chemistry, Univ. California, Riverside, CA 92521.
Other Locations:	Dept. Chem. Eng., Carnegie Mellon Univ., Pittsburgh, PA 15213 Dept. Chemistry, Univ. Wisconsin, Milwaukee, WI 53211.
Contact Information:	email: zaera@ucr.edu Phone: (951) 827-5498, Fax: (951) 827-3962
Project Starting Year:	2003

Abstract

The overall research goal of this project is to determine the mechanisms by which enantioselectivity can be bestowed on heterogeneous catalysts. Specifically, chirality is to be imparted to achiral surfaces either by exposing chiral planes or by using chiral modifiers.

The significant achievements and results can be summarized as follows:

4.1.1 Naturally chiral surfaces

- Completion of a systematic study of the enantiospecific desorption kinetics of R-3-methylcyclohexanone (R-3-MCHO) on 9 achiral and 7 chiral Cu surfaces with crystallographic orientations that span the stereographic triangle.
- Discovery of super-enantioselective tartaric acid decomposition as a result of a chiral surface explosion mechanism on Cu(643)$^{R\&S}$.
- Initial observation of the enantiospecific desorption of R- and S-PO from Cu(100) imprinted with {3,1,17} facets by L-lysine adsorption.

4.1.2 Templated chiral surfaces

- Initial observation of the enantiospecific desorption of R- and S-PO from Pt(111) and Pd(111) modified with a variety of chiral templates.
- Demonstrated enantioselective separation of racemic PO on chemically synthesized chiral Au nanoparticles.
- Discovery of zwitterionic adsorption states of amino acids on Pd(111).
- First structure determinations of adsorbed amino acids based on combined theory and electron diffraction methodology.

4.1.3 One-to-One interactions

- Systematic study of the influence of solution properties on the adsorption of modified cinchonas alkaloids onto Pt surfaces.
- Correlation of cinchona adsorption with catalytic activity, as affected by concentration, the nature of the solvent, and dissolved gases in the liquid phase.
- Determination of cinchona orientation on Pt surfaces using FT-IRAS
- Measurement of enantioselective chemisorption on 1-(1-naphthyl) ethylamine (NEA) modified surfaces

Potential impact in science and technologies of interest to DOE: The basic knowledge generated from the studies being carried out by our research team is expected to advance the development of heterogeneous chiral catalysis, and in more general terms, selectivity in catalysis.

Technical Report

Results

Naturally chiral surfaces

R-3-methylcyclohexanone on Cu(*hkl*)

By far the most carefully studied combination of chiral adsorbate and naturally chiral surface is R-3-methylcyclohexanone (R-3-MCHO, figure 4) on the Cu(643)$^{R\&S}$ surfaces. The enantiospecific desorption energies, ΔE_{des}, of R-3-MCHO on Cu(643)$^{R\&S}$ have been measured by Gellman using temperature programmed desorption (TPD). Figure 4 shows the TPD spectra of R-3-MCHO desorbing from the Cu(643)$^{R\&S}$ surfaces. Careful study of R-3-MCHO TPD from Cu(111), Cu(221) and Cu(533) surfaces has shown that the three desorption features in figure 4 can be assigned to R-3-MCHO desorbing from the terraces (230 K), straight step edges (345 K) and kinks (385 K). As shown in the expanded section of the TPD spectra, desorption of R-3-MCHO from the R- and S-kinks is enantiospecific. The difference in the peak desorption temperatures is $\Delta T_p = 3.5 \pm 0.8$ K and corresponds to an enantiospecific difference in desorption energies of $\Delta\Delta E_{des} = 0.97 \pm 0.25$ kJ/mole [15, 16, 19]. Fourier Transform Infrared Reflection Absorption Spectra (FT-IRAS) of R-3-MCHO on Cu(643)$^{R\&S}$ reveal that this enantiospecific interaction also manifests itself in differences in the orientations of R-3-MCHO adsorbed at the R- and S-kinks on the Cu(643)$^{R\&S}$ surfaces [21].

Over the past grant period Gellman has completed an exhaustive study of the adsorption and desorption of R-3-MCHO on a large set of Cu surfaces that span all regions of the stereographic projection [15, 16, 35, 36]. This includes nine achiral surfaces and seven chiral surfaces (figure 5): Cu(643)$^{R\&S}$, Cu(653)$^{R\&S}$, Cu(821)$^{R\&S}$, Cu(17,5,1)$^{R\&S}$, Cu(651)$^{R\&S}$, Cu(13,9,1)$^{R\&S}$ and Cu(531)$^{R\&S}$. The TPD spectra from all of these surfaces exhibit qualitatively the same types of features as those revealed in figure 4A for TPD from the Cu(643)$^{R\&S}$ surface; desorption from terraces, steps edges, and kinks.

Comparisons of the desorption kinetics of R-3-MCHO from the R- and S- kinks of an enantiomeric pair of chiral Cu(*hkl*)$^{R\&S}$ surfaces can be used to estimated the enantiospecific difference in desorption energies, $\Delta\Delta E_{des}$. Figure 5 indicates the values of $\Delta\Delta E_{des}$ observed from these chiral surfaces and the fact that the magnitudes of these are all in the range $\Delta\Delta E_{des} \sim 0.5 - 1.0$ kJ/mole. As a point of reference, this corresponds to an enantiospecific difference in desorption rates of ~20 - 50% at 300 K. Many successful chiral chromatographic separations have been base upon enantiospecific differences in adsorption energetics of $\Delta\Delta E_{des} < 1$ kJ/mole [15, 18]. In looking at figure 4, it is important to note also that the sign of $\Delta\Delta E_{des}$ reverses within the stereographic projection, indicating that enantioselective adsorption of R-3-MCHO is influenced by subtle details of the surface structure. This sign reversal has also been seen in DFT calculations by Sholl for the chemisorptions of small chiral species on Cu surfaces sampling the stereographic triangle [63].

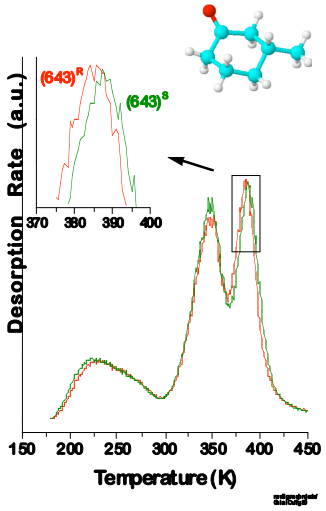

Figure 4. TPD of R-3-methylcyclohexanone from the Cu(643)$^{R\&S}$ surfaces. The three desorption features arise from molecules desorbing from the terraces (230 K), step edges (345 K) and kinks (385 K). Expansion of the TPD spectra from the R- and S-kinks, reveals enantiospecific desorption temperatures, $\Delta T_p = 3.5$ K.

2-Butyl groups on Cu(643)$^{R\&S}$ and Cu(531)$^{R\&S}$

In addition to enantiospecific desorption, Gellman has shown that reactions of chiral adsorbates are enantioselective on naturally chiral metal surfaces. Using R-2-iodobutane and S-2-methyl-iodobutane his group has prepared R-2-butyl and S-2-methylbutyl groups on the Cu(643)$^{R\&S}$ and Cu(531)$^{R\&S}$ surfaces [37, 38]. R-2-iodobutane reacts by the mechanism shown in Figure 6 to produce a set of products by reaction steps including desorption (to produce R-2-iodobutane), de-iodination (R-2-butyl), β-hydride elimination (butenes), and hydrogenation (butanes). S-2-Methyl-iodobutane reacts via these same elementary reaction steps but produces a different set of products. TPD studies in Gellman's laboratory have determined the enantioselectivities of the reaction yields. This work has demonstrated that these reactions are enantioselective and that the enantioselectivity is greater on the Cu(531)$^{R\&S}$ surfaces than on the Cu(643)$^{R\&S}$ surfaces.

Enantioselective explosion of tartaric acid on Cu(643)$^{R\&S}$

Enantiospecific differences in the reaction energetics of chiral molecules tend to be small. The difference of $\Delta\Delta E_{des} \approx 1$ kJ/mole for R-3-MCHO on Cu(643)$^{R\&S}$ is typical [15, 16, 19]. The subtlety is manifested in the TPD spectra of figure 4, which reveal a 3.5 K shift in peak temperature between desorption peaks that have intrinsic peak widths of ~30 K. The obvious way to achieve higher enantioselectivity is to find processes with much larger enantiospecific reaction energetics; an enantioselectivity of ×100 at 300 K requires an enantiospecific difference in reaction energetics of $\Delta\Delta E \approx 10$ kJ/mole. Alternatively, selectivities are also controlled by reaction rate laws, and this provides a route to enhanced enantioselectivity.

In recent work, Gellman has examined surface reactions that occur by 'explosive' mechanisms with highly non-linear rate laws. Such reactions mechanisms were first identified by Madix *et al.* in the mid 1970's during formic acid decomposition on Ni(110) [196]. They manifest themselves in the

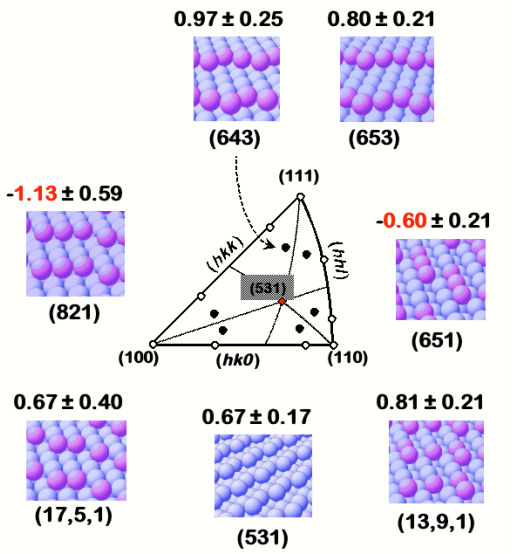

Figure 5. The stereographic triangle of fcc surfaces. R-3-MCHO desorption has been studied on all 16 surfaces indicated by points in the stereographic triangle. The seven surfaces in the interior of the triangle are chiral. The enantiospecific desorption energies, $\Delta\Delta E_{des} = \Delta E^{S}_{des} - \Delta E^{R}_{des}$, on the naturally chiral surfaces are indicated above the images of the ideal surface structures.

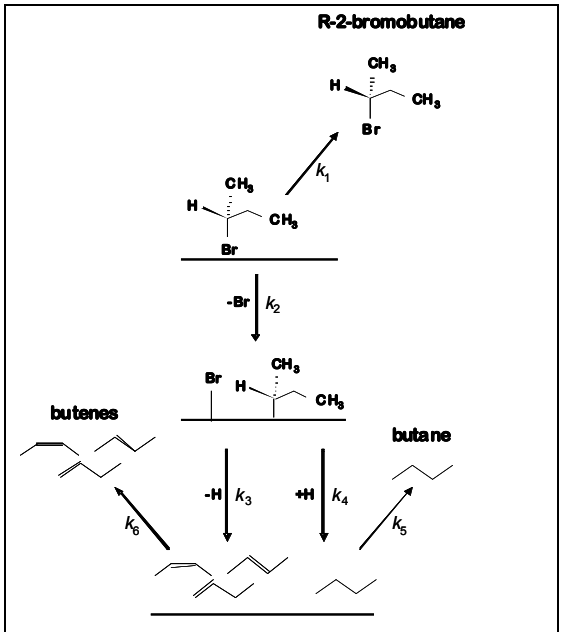

Figure 6. Reaction mechanism of R-2-butane on Cu(643)$^{R\&S}$ and on Cu(531)$^{R\&S}$ surfaces. The yields of the various products are enantiospecific. The Cu(531)$^{R\&S}$ surfaces are more enantioselective that the Cu(643)$^{R\&S}$ surfaces [37, 38].

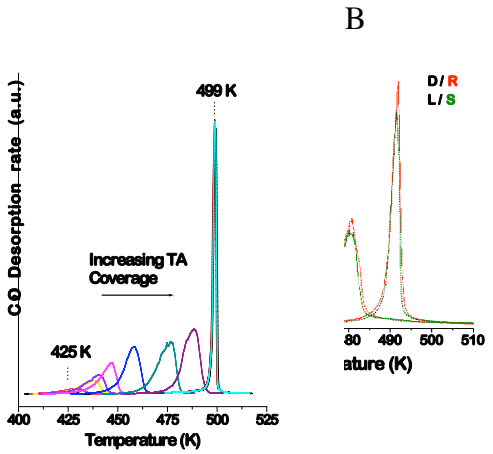

Figure 7. Enantiospecific explosion of tartaric acid on Cu surfaces. A) TPD spectra of tartaric acid decomposition on Cu(110) following increasing initial exposures to tartaric acid. The peak temperatures increase with initial coverage and then converge at saturation coverage to a very narrow feature at 499 K. B) The explosive decomposition of tartaric acid on Cu(643)$^{R\&S}$ exhibits super-enantioselectivity. The ratio of decomposition rates at 480 K is ~30.

form of very narrow desorption peaks during TPD experiments. The decomposition of tartaric acid on Cu(110) has been shown to occur by an explosive mechanism [197, 198]. It has been suggested that the decomposition mechanism is one that requires the presence of an empty site and therefore that the rate law is

$$r = k\,\theta \cdot (1\text{-}\theta). \qquad (1)$$

As a consequence, the reaction becomes autocatalytic when initial coverages approach $\theta_0 = 1$. Figure 7A shows the TPD of tartaric acid decomposition on the Cu(110) surface obtained for initial coverages varying from $\theta_0 = 0.1$ to ~1. They reveal the extremely narrow desorption features characteristic of explosive decomposition at saturation coverages. Initial attempts at modeling these TPD spectra suggest that the rate law is in fact third-order,

$$r = k\,\theta \cdot (1\text{-}\theta)^2. \qquad (2)$$

This highly non-linear rate law leads to surface reactions occurring over very narrow temperature ranges and with extremely high enantioselectivities, in spite of the fact that the difference in peak temperature, ΔT_p, might be quite small.

Recently, Gellman's lab has made a significant breakthrough by exploiting explosive surface reaction kinetics as a means of enhancing enantioselectivity on naturally chiral metal surfaces. Figure 7B shows the TPD spectra of D- and L-tartaric acid on the Cu(643)$^{R\&S}$ surfaces. These display true diastereomerism. Serendipitously, the peak reaction temperatures for decomposition differ by ~12 K between the two pairs of TPD spectra. More importantly, the enantioselectivity of the reaction rates at 480 K is a factor of ×30, translating into an *ee* ≈ 94%! This is more than an order of magnitude greater than any other enantioselectivity observed on a naturally chiral surface and arises from the highly non-linear process leading to the very narrow TPD peaks.

Prior results – Templated chiral surfaces

R- and S-2-butoxide templated Pd(111)

The strategy for understanding the way in which chiral modifiers are able to impart chirality to surfaces is based on measuring enantioselective adsorption of chiral probe molecules on chirally modified surfaces. The methodology, first developed by Tysoe, was demonstrated by

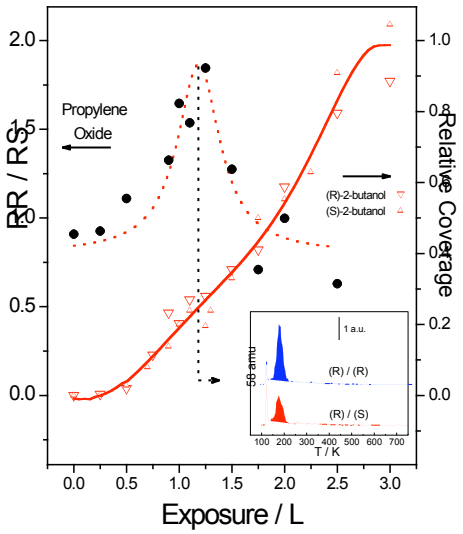

Figure 9. Plot of the relative coverages of (S)-and (R)-2-butoxide as a function of exposure on Pd(111) (red open symbols, right axis), and of the ratio of the coverages of (R)- to (S)-propylene oxide (RR/RS) adsorbed on (R)-2-butoxide-covered Pd(111) (black filled circles, left axis), both as a function of 2-butanol exposure. Shown in the inset are typical propylene oxide desorption spectra from 2-butoxide-covered Pd(111) surfaces. This figure highlights the enantioselective preference that the surface exhibits for the adsorption of (R)- rather than (S)-propylene oxide on chiral sites made by adsorption of (R)-2-butoxide.

modifying Pd(111) surfaces with either R- or S-2-butanol and then exposing the modified surfaces to fixed exposures of R- or S-PO. Subsequent measurement of the coverage of adsorbed PO revealed that the uptake of PO is enantiospecific (Figure 9) [42, 48, 55]. In this case, PO was selected as a probe molecule because it adsorbs on Pd(111) without decomposing and because the monolayer coverage can be determined using FT-IRAS and TPD [151]. 2-Butanol was selected for initial study as a template because it contains an anchoring group (the hydroxyl) and a chiral center. 2-Butanol adsorbs molecularly on Pd(111) at low temperatures (~80 K) but then deprotonates on heating to form 2-butoxide [44] which, at higher temperatures (above ~200 K) undergoes a β-hydride elimination reaction to form 2-butanone (eliminating the chiral center).

Exposure of the Pd(111) surface modified by adsorption of R- or S-2-butanol to R- or S-PO results in an enantiospecific uptake of PO, but only over a narrow coverage range of the adsorbed 2-butanol (figure 9). By measuring the enantioselective uptake of PO on Pd(111) surfaces with different proportions of adsorbed 2-butanol and 2-butoxide species, it was demonstrated that the enantioselectivity correlated with the presence of 2-butanol on the surface (rather than 2-butoxide) indicating that hydrogen-bonding interactions between the 2-butanol and PO are central to imparting enantioselectivity [53, 55]. This was confirmed by showing that adsorption of PO is not enantioselective when the Pd(111) surface is modified by 2-butoxide only (prepared by adsorbing 2-butanol on oxygen coverage Pd(111)).

Various chiral templates on Pd(111), Pt(111), Cu(100) and Cu(111)

Systematic modification to the molecular structure and functionality of the chiral template molecules has been used to explore the interactions that lead to enantioselective uptake of chiral probe molecules such as PO. The results of such studies on Pd(111) are summarized in figure 10 which depicts the maximum (versus chiral template coverage) enantiospecific ratios, ER, for R- and S-PO uptake on Pd(111) surfaces modified with a variety of template molecules. Replacing the hydroxyl group of 2-butanol with a carboxylate group (2-methyl butanoic acid) results in the formation of 2-methyl butanoate on the Pd(111) surface. As a chiral modifier, this imparted no enantioselectivity to the uptake of PO. In view of Tysoe's findings with 2-butanol and 2-butoxide, this lack of enantioselectivity can be understood to arise from the lack of hydrogen-bonding interactions between PO and the 2-methyl butanoate, further emphasizing the

importance of hydrogen bonding for enantioselective uptake of PO. Interestingly, however, similar experiments by Zaera on platinum substrates revealed that 2-methyl butanoate could act as a weak chiral modifier for PO uptake [52]. This intriguing influence of the substrate is also seen when using 1-(1-naphthyl) ethylamine (NEA), a putative one-to-one modifier (figure 11). When using NEA as the chiral modifier, PO uptake is not enantioselective on Pd(111) [57], whereas PO uptake is enantioselective on Pt(111) [43]. In related experiments using templated Cu(100) and Cu(111) Gellman has also observed influences of the substrate on enantioselective uptake of PO. This intriguing dependence of enantioselectivity on the nature of the substrate clearly warrants further investigation.

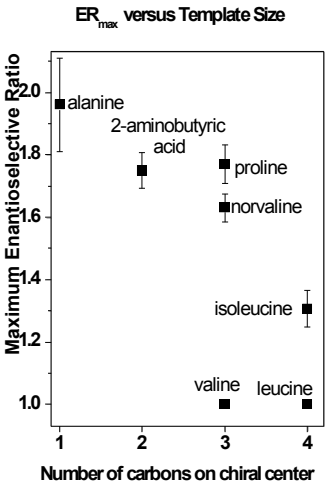

Figure 10. Maximum enantiospecific uptake ratios of R- and S-PO on Pd(111) surfaces modified by the template molecules indicated.

Structure and enantioselectivity of amino acid templates

Not surprisingly, the structure of the templating agent influences the enantioselective adsorption of PO. One can introduce a hydrogen-bonding site into 2-methylbutanoate by substituting an amine group for either the methyl or the ethyl groups, thus creating amino acids; 2-aminobutyric acid or alanine, respectively. As seen in figure 10, this imparts enantioselectivity to the uptake of R- or S-PO. As a consequence, Tysoe and Sholl have explored the surface chemistry and structure of amino acids on Pd(111) [46, 49-51, 68, 71] and Gellman has studied amino acids on Cu surfaces. XPS reveals that the amino acids glycine, alanine and proline are present in both their zwitterionic (R-C(H)(NH_3^+)CO_2^-) and anionic (R-C(H)(NH_2)CO_2^-) forms on Pd(111) [50, 51], while on other surfaces, notably Cu they are present exclusively in the anionic form. Sholl's recent DFT calculations [46] suggest that the zwitterionic form is metastable on the Cu surface. This suggests that the zwitterionic form is initially deposited from the gas phase and then reacts to yield the anionic form on heating. In the case of more reactive Pd surfaces, the conversion to the anionic form competes with the decomposition of the adsorbed amino acid, which occurs a little above ~300 K [46, 49-51].

Amino acids form enantioselective chiral templates for PO adsorption on several surfaces. As indicated in figure 10, the enantioselectivity on Pd(111) decreases with increasing *n*-alkyl chain length, while amino acids with secondary alkyl chains show no enantioselectivity for PO uptake. LEED and FT-IRAS experiments have been performed by Tysoe to determine the structures of amino acids on Pd(111) surfaces. These are extremely challenging experiments not only because of the heterogeneous nature of the template layer (containing both zwitterionic and anionic species), but also because adsorbed amino acids decompose rapidly in the electron beam and their infrared absorbencies are extremely small. Tysoe has, nevertheless, obtained LEED I/E curves for glycine, alanine and proline on Pd(111) using a

Figure 11: Structure of 1-(1-naphthyl) ethylamine (NEA). A chiral modifier related in structure to the cinchina alkaloids.

picoLEED system in collaboration with Professor Carol Hirschmugl at UWM. These I/E curves are currently being analyzed by Dr. Georg Held at the University of Reading, UK. Adsorption geometries are being refined using initial structures determined by Sholl from DFT calculations [46]. Tysoe has recently collected the FT-IRAS spectra of alanine and glycine on Pd(111) and the spectra are consistent with the XPS in that they reveal the presence of both zwitterionic and anionic species on the Pd(111) surface. Preliminary scanning-tunneling microscopy (STM) images of proline and alanine on the Pd(111) surface are providing information on the distribution of the amino acids on the surface. These combined efforts of Tysoe and Sholl are providing a clear picture of the structure and conformations of the amino acids on Pd(111) which can ultimately be correlated with their enantioselectivity for the adsorption of probe molecules.

Enantioselective reactions on templated chiral surfaces

Templated chiral surfaces can induce enantioselectivity into surface reactions. This was demonstrated by Tysoe in a study of the dehydrogenation reactions of R- and S-2-butanol on L-proline-modified Pd(111) [57]. In that case, 2-butanol was used as a chiral probe rather than a modifier. On the clean Pd(111) surface, 2-butanol adsorbs irreversibly; during heating it converts stoichiometrically to 2-butoxide and then undergoes a β-hydride elimination reaction to form 2-butanone. An L-proline template on the Pd(111) surface modifies the surface chemistry of 2-butanol such that the major fraction adsorbs and desorbs reversibly with only a small fraction reacting to form 2-butoxide. The enantioselectivity, defined as the ratio of S-2-butanol coverage to R-2-butanol coverage formed following exposure to 2-butanol at ~100 K, varies with the L-proline coverage and reaches a maximum of ~1.2 at an L-proline coverage of ~0.2. The hydrogenation of 2-butoxide back to 2-butanol by co-adsorbed deuterium is also enantioselective in the presence of the L-proline modifier and reaches a maximum of ~1.9 at an L-proline coverage of ~0.2. Both adsorption and the subsequent reaction of the adsorbed species are enantioselectively.

Substrate effects on the enantioselectivity of templated surfaces

The nature of the substrate (Pd *vs.* Pt *vs.* Cu, for example) influences the enantioselective interaction between a given chiral template and chiral probe. Tysoe, Zaera and Gellman have shown that the enantioselective uptake of R- or S-PO on R- or S-2-butanol templated surfaces differs among Pd(111), Pt(111), Cu(111) and Cu(100). Zaera and Tysoe have also demonstrated differences in the enantioselective adsorption of PO on Pt(111) and Pd(111) modified with 2-methyl butanoic acid and with NEA [43, 57, 85].

In order to further explore substrate effects on the surface chemistry of chirally templated surfaces, the co-adsorption of R- and S-PO probe with an R-2-butanol template was studied by Tysoe using a dilute Au/Pd(111) alloy containing ~8% Au [47]. The surface chemistry of PO and 2-butanol on the alloy is quite different from that on clean Pd(111). On the Au/Pd(111) alloy surface, a portion of the PO decomposes to form CO and ethylidyne ($\equiv C\text{-}CH_3$); on clean Pd(111), PO adsorbs reversibly. Furthermore, 2-butanol reacts to form 2-butoxide species on the alloy on heating to ~170 K. At ~250 K, 2-butoxide either rehydrogenates to form 2-butanol or undergoes a β-hydride elimination reaction to yield 2-butanone. Co-adsorption of R-2-butanol with R-PO or S-PO leads to enantioselective (*ee* of ~14%) 2-butanone formation that is greater in the presence of S-PO than in the presence of R-PO. Because the 2-butanone formation occurs at slightly lower temperatures than the rehydrogenation to 2-butanol (~210 K versus 240 K), there is an enantioselective enrichment of surface 2-butoxide species such that the subsequent 2-

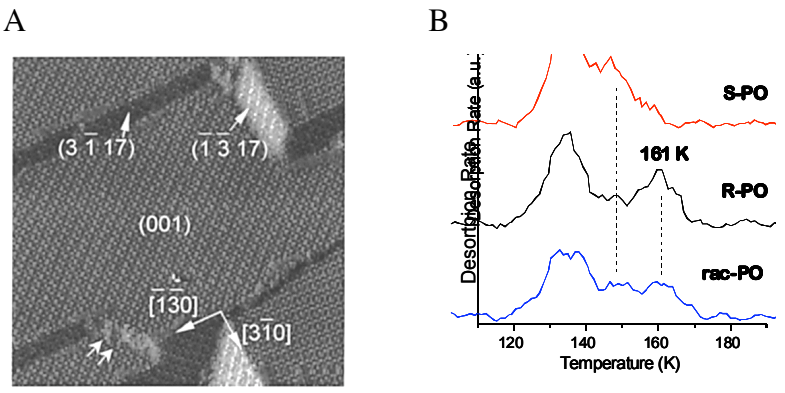

Figure 12. A) An STM image of a Cu(100) surface modified by the L-lysine. Adsorption has caused step bunching to form a homochiral set of {3,1,17} facets [192]. B) TPD of ~0.01ML of R- and S- PO from the L-lysine modified Cu(100) surface. The peak at 135 K is characteristic of desorption of PO on lysine. The peaks at 147 and 161 K are due to PO interacting with the Cu surface and the lysine monolayer. The enantiospecific difference in peak desorption temperatures is ~15 K.

butanol formation is also enantioselective. The resulting *ee* values for the formation of 2-butanol from the remaining 2-butoxide species depend strongly on the initial 2-butanol coverage, varying from a few percent at moderate coverage, to *ee* ≈ 100 % at low initial 2-butanol coverages [47].

PO on L-lysine/Cu(100) – templated or imprinted chiral surface?

One of the most interesting enantiospecific interactions of amino acids with achiral surfaces is the example of L-lysine on Cu(100). Several studies of amino acids on Cu(100) surfaces have used STM to show that amino acids cause gross reconstruction, leading to the formation of {3,1,17} facets [189, 192, 193]. These are naturally chiral planes, but in the presence of glycine or L-alanine, reconstruction leads to equal fractions of the $\{3,1,17\}^R$ and $\{3,1,17\}^S$ facets. However, Zhao *et al*. have shown that when L-lysine is adsorbed on the Cu(100) surface it leads to the formation of a homochiral set of $\{3,1,17\}^R$ facets (figure 12A) [192, 193]. In principle, this result indicates that L-lysine can be used to *imprint* natural chirality onto an achiral Cu surface. The implication is that imprinting could be used as a chemical means of creating high surface area materials that expose naturally chiral planes.

Gellman has explored the adsorption of R- or S-PO on Cu(100) surfaces modified by adsorption of L-lysine. At high coverages of adsorbed PO there is no observable enantiospecific adsorption; most PO desorbs from the surface as though it is adsorbed in a multilayer film (135 K). At low PO coverages, however, PO desorption is highly enantiospecific. Figure 11B shows the TPD spectra of R- and S-PO at a coverage of ~1% on the L-lysine modified Cu(100) surfaces. The enantiospecific difference in the desorption peak temperatures is ~15 K, larger than that observed in any other such system. The fact that this only occurs for a small fraction of a monolayer of PO is consistent with Zhao's observation that only small fraction of the Cu(100) surface reconstructs to {3,1,17} planes [192, 193]. Gellman will explore the adsorption of R- and S-PO on $Cu(3,1,17)^{R\&S}$ with and without adsorbed L-lysine and on Cu(100) surfaces modified by D-lysine.

Templated Au nanoparticles

As another route to preparing chiral surfaces in high area, Gellman has collaborated with Dr. Nisha Shukla (at CMU) at in the preparation of chiral Au nanoparticles. Dr. Shukla has synthesized Au nanoparticles modified by adsorbed L- or D-cysteine. As shown in figure 13, these Au nanoparticles adsorb PO enantioselectively. Addition of racemic PO to a solution of L-cys/Au nanoparticle results in the rotation of polarized light. As the concentration of racemic PO is increased, the rotation of light increases. Light is rotated in the opposite direction during

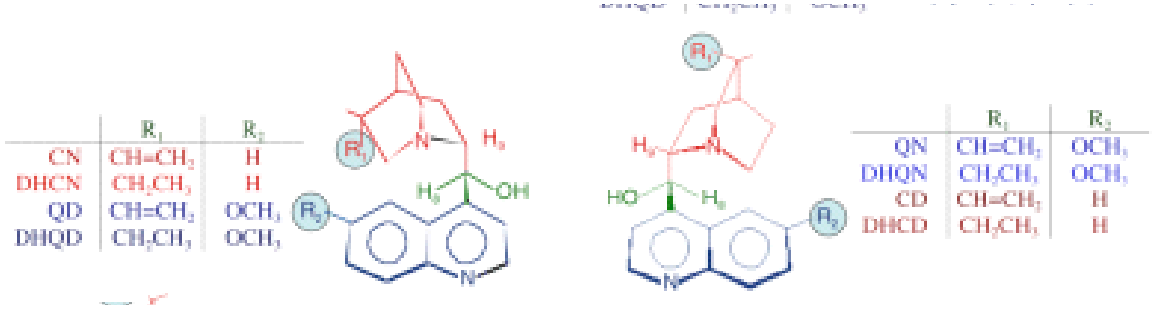

Figure 14. Structure of the cinchona alkaloids: cinchonidine, CD; cinchonine, CN; quinine, QN; quinidine, QD; dihydrocinchonidine, DHCD; dihydrocinchonine, DHCN; dihydroquinine, DHQN; and dihydroquinidine, DHQD. These form pairs of 'near' enantiomers that differ only in nature of the peripheral functional groups on the quinuclidine ring (R_1 = H or OCH_3) and quinoline ring (R_2 = $CH=CH_2$ or CH_2CH_3).

addition of racemic PO to solutions of D-cys/Au nanoparticles. This is the result of enantioselective adsorption of PO onto the chiral Au nanoparticles. The enantiospecific origins of this effect have been confirmed by showing that there is no rotation of polarized light during addition of racemic PO to a solution of Au nanoparticles modified by racemic cysteine. What remains to be done is quantification of the degree of the PO separation, and the effects of substrate and chiral modifier on the degree of separation.

Prior results – One-to-one chiral interactions

Orientation of cinchonidine on Pt

In order to understand the one-to-one modifier-reactant interaction mechanisms for imparting enantioselectivity, Zaera has used infrared spectroscopy to characterize the adsorption of cinchonidine and other related modifiers on Pt surfaces from solution [82, 89, 91]. Vibrational assignments for the cinchonidine were first made using a combination of experimental spectroscopic measurements and *ab initio* computational methods [88, 91]. It was found that the geometry of the cinchonidine modifier on Pt is very sensitive to its concentration in solution. At low and intermediate concentrations, the cinchonidine is adsorbed with the quinoline ring parallel to the surface; however, at high concentrations, the ring is tilted away from the surface. The optimum enantioselectivity occurs under conditions consistent with a modifier adsorption geometry having the quinoline ring parallel to the surface [81, 96].

Cinchona adsorption onto Pt – solution effects

The influence of dissolved gases on the adsorption of cinchonidine from CCl_4 solutions onto polycrystalline Pt surfaces was characterized using FT-IRAS [93]. Most of the gases studied (Ar, N_2, O_2, air and CO_2), have no detectable influence on cinchonidine adsorption on Pt. On the other hand, H_2 plays a unique role, initially accelerating the uptake kinetics of cinchonidine, but later displacing some of the adsorbed cinchonidine from the Pt surface.

There are also a number of reports of the impact of solvent on the enantioselectivity of the Orito reaction. The solvent was found to have a strong influence on the adsorption of cinchonidine on the catalyst surface [92]. In particular, the polarity of the solvent was found to influence the kinetics of cinchonidine desorption into solution in a manner that correlated well with the solvent influence on the enantioselectivity of the cinchonidine modified Pt catalyst. Cinchonidine adsorbs irreversibly on Pt from non-polar solutions such as cyclohexane, but can be easily removed by more polar solvents such as CH_2Cl_2. The evolution of the adsorbed

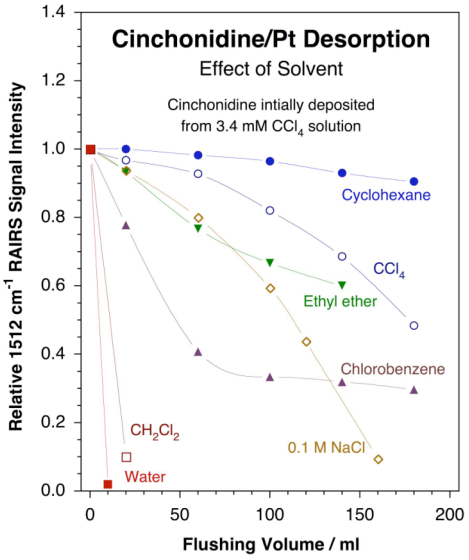

Figure 15. Desorption of adsorbed cinchonidine from a Pt surface into different solvents as a function of rinsing volume. In these experiments the cinchonidine was first adsorbed from a CCl_4-saturated solution, and then flushed with sequential 20 ml aliquots of the stated solvents. The coverage of the adsorbate remaining on the surface was determined in-situ by following the infrared absorption signal at 1512 cm^{-1}, which corresponds to an in-plane deformation of the quinoline ring. The data show that the desorption kinetics are very sensitive to the nature of the solvent, varying from fast desorption in water and dichloromethane to irreversible adsorption in cyclohexane and other alkanes. This trend correlates well with the chirality-imparting ability of cinchonidine for enantioselective hydrogenation reactions on Pt catalysts.

cinchonidine overlayer on Pt during flushing with different solvents is illustrated in figure 15. The behavior observed in Zaera's studies correlates well with the solubility of cinchonidine in different solvents and with the activity and enantioselectivity of the cinchonidine/Pt catalyst for the Orito reaction in these solvents.

In general, we have concluded that the enantioselective properties of the cinchonidine/Pt catalyst are defined by the adsorption geometry of the chiral modifier, and that those in turn are influenced by details of the reaction system, such as the concentration of the modifier in solution, the type of solvent, and the nature of the gasses dissolved in the liquid phase [82].

Cinchona structure – impact on adsorption

Having explored the effects of solution on cinchonidine adsorption on Pt, the next avenue of investigation was to understand the effects of the modifier's molecular structure on its adsorption properties and on its ability to impart enantioselectivity to catalytic processes. A comparative study was carried out using cinchonidine, cinchonine, quinine, quinidine, and the dihydro analogs of those four molecules (figure 14). Interesting trends in adsorption equilibria were observed, as illustrated by the data in figure 16. The adsorption equilibrium constants (K_{ads}) were found to follow the sequence cinchonine > quinidine > cinchonidine > quinine [94]. Some of this ordering can be explained by differences in solubility, but quinidine displays a much larger K_{ads} than expected based on its large relative solubility; bonding to the surface must also play a role in determining the trends in K_{ads}.

Using FT-IRAS, it was determined that each of the cinchona alkaloids binds differently on Pt at saturation coverages; while the quinoline ring of cinchonidine tilts along its long axis to optimize π-π intermolecular interactions, in cinchonine it tilts along the short axis and bonds through the lone electron pair of the nitrogen atom instead. Both quinine and quinidine exhibit additional bonding to the surface via the methoxy oxygen atom [91]. Perhaps a more surprising result from this work is the fact that cinchonine displays a higher K_{ads} than cinchonidine, quinine or quinidine in spite of the fact that, according to previous work, it can be readily displaced from the surface by any of those other cinchona alkaloids [95]. A full explanation of these observations requires consideration of the solvent interaction with the adsorbed species.

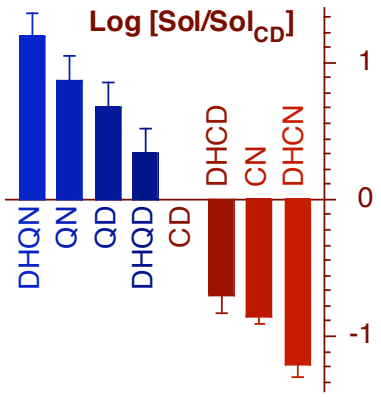

Figure 17. Solubilities of different cinchona relative to those of cinchonidine (CD). The numbers reported are averages over the values measured in more than 30 solvents, with error bars that correspond to 95% confidence intervals. No significant variations in relative solubilities were observed as a function of the nature of the solvent, implying that the changes observed are intrinsic to the structure of the cinchona. 2-D NMR experiments lead us to propose a connection between those changes and variations in the configurations available to each compound, which are in turn affected by the peripheral functional groups in the quinuclidine and quinoline rings, R_1 and R_2 respectively in figure 13.

The differences observed among the different cinchona alkaloids, both in their adsorption properties and in their behavior in solution, were deemed to arise from intrinsic molecular properties associated with their structure: the relative solubilities of the different cinchona alkaloids remain approximately constant in different solvents (figure 16). Correlations between the conformations of cinchona's and their chemical behavior have already been identified in a few cases, but not properly explained. Preliminary NMR and DFT data suggest that the most stable configuration of each molecule may be determined by the steric effects exerted by the peripheral functional groups (vinyl, methoxy) bonded to the quinuclidine and quinoline rings. This behavior may account for the reported differences in catalytic enantioselectivities observed when using cinchonidine and cinchonine as chiral modifiers. The role of these peripheral groups in defining the behavior of cinchona's in solution, their adsorption, and their ability to impart chirality in catalytic systems, is one of the directions of research proposed for the next funding period of this project. An improved understanding of this effect will lead to the preparation of specific new modifiers by changing their peripheral groups to tune their catalytic behavior.

Substrate effects on one-to-one interactions: Pt(111) vs. Pd(111)

The enantioselectivity of the Orito reaction catalyzed by Pt is greater than when it is catalyzed by Pd [97, 98, 154, 168, 205, 206]. Tysoe and Zaera have explored the origins of this difference. Rather than using cinchonidine which is difficult to study in UHV, their work has made use of the modifier NEA (figure 11) which has also been shown to be an effective chiral modifier for the Orito reaction [49, 206-208]. The effect of substrate has been explored by studying the enantioselective adsorption of R- and S-PO on NEA modified Pt(111) [43, 57] and Pd(111) [57]. The adsorption of PO exhibits no detectable enantioselectivity on

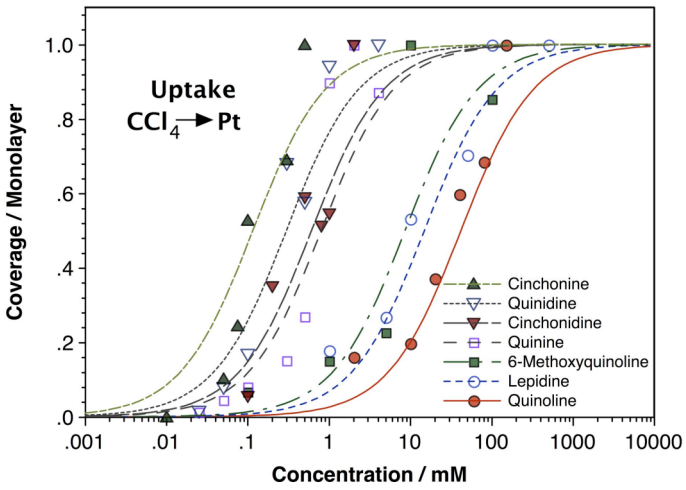

Figure 16. Adsorption isotherms for several cinchona and related compounds from solution onto a platinum surface, as determined by in-situ infrared spectroscopy detection.

NEA-modified Pd(111) but readily measurable enantioselectivity on Pt(111).

R- and S-2-butanol have also been used as a chiral probe of the NEA modified Pd(111) surface, and, in contrast to PO, do exhibit enantioselective adsorption. At an NEA coverage of 0.055 ML the 2-butanol can interact with both the Pd(111) substrate and the NEA modifier and adsorbs with ER ~ 2. On a Pd(111) surface with a saturation overlayer of NEA (~0.1 ML) the 2-butanol adsorbs on top of the NEA modifier layer with ER ~ 1.8 (figure 17). Infrared spectroscopy reveals that the interaction between 2-butanol and the NEA causes the NH_2 group of NEA to reorient to facilitate its hydrogen bonding interactions with the 2-butanol. The heat of adsorption of 2-butanol on NEA modified Pd(111) is ~35 kJ/mol which is typical of –OH…NH_2 hydrogen bond strengths [209]. This is an example where it is the probe molecule and not the modifier the one that makes a difference in he degree of enantioselectivity observed. This synergy between the modifier and the probe is to be explored in more detail.

Methyl lactate and methyl pyruvate on NEA modified Pd(111)

In order to mimic the Orito reaction Tysoe has begun to explore the interaction of methyl lactate (the hydrogenation product of methyl pyruvate) with NEA-modified Pd(111). As a precursor to these experiments, the surface chemistry of methyl pyruvate and methyl lactate has been studied on Pd(111). At lower coverages, methyl pyruvate adsorbs with its molecular plane parallel to the surface, while at saturation coverage it adsorbs with its molecular plane perpendicular to the surface. During heating, the perpendicular methyl pyruvate desorbs at lower temperatures than the parallel form so that two desorption peaks are observed in TPD experiments, a low-temperature state for perpendicular methyl pyruvate desorption and the high-temperature state from flat-lying methyl pyruvate that forms as the surface coverage decreases. At higher temperatures, a portion of the flat-lying methyl pyruvate decomposes. Methyl lactate either desorbs from Pd(111) or dehydrogenates to form flat-lying methyl pyruvate, which subsequently decomposes in an identical manner to that found for flat-lying methyl pyruvate on Pd(111).

Preliminary TPD experiments have been performed to examine the effect of NEA on the chemistry of methyl lactate. Initial data reveal enantiospecific dehydrogenation to form methyl pyruvate, the reverse of the Orito reaction. In this case, the R- or S-NEA modified surface is saturated with R- or S-methyl lactate and the desorption of (flat-lying) methyl pyruvate monitored using TPR. The yield of methyl pyruvate decreases with increasing NEA coverage as the surface becomes blocked. However, the yield of methyl pyruvate is enantioselective; there is an NEA coverage regime in which no methyl pyruvate is formed when S-methyl lactate is adsorbed on an R-NEA covered surface while methyl pyruvate *is* detected from an S-NEA-covered surface indicating an *ee* that approaches 100%. These preliminary data indicate that it will be possible to explore the enantiospecific hydrogenation reactions on NEA-modified surfaces by studying its microscopic reverse reaction, dehydrogenation. Further experiments will be carried out to corroborate this conclusion.